UNIVERSITÀ
DEGLI STUDI
FIRENZE

DOTTORATO DI RICERCA IN SCIENZE CLINICHE

CICLO XXVII

Coordinatore Prof. Laffi Giacomo

$CD4^+$ intrahepatic lymphocytes drive liver inflammation via impaired regulatory pathways in a murine model of Crohn's-like ileitis

Settore Scientifico Disciplinare MED/12

Dottorando
Dott. Omenetti Sara

Tutore
Prof. Pizarro T. Theresa

Coordinatore
Prof. Laffi Giacomo

Anni 2012/2014

Table of contents

Introduction

Inflammatory bowel disease (IBD) is a chronic inflammatory condition of the intestine, comprised primarily of two diseases: ulcerative colitis (UC) and Crohn's disease (CD). The localization and pattern of disease are different. CD can typically affect any location throughout the entire gastrointestinal tract in a discontinuous manner, most commonly in the terminal ileum, with inflammation that is typically transmural and often granulomatous. Conversely, UC localizes to the rectum and colon in a confluent pattern and is limited to the mucosa and submucosa.

Extra-intestinal manifestations of IBD

IBD is frequently associated with extra-intestinal manifestations and autoimmune disorders. IBD-associated extra-intestinal manifestations can involve many organ systems, where they can follow the course and timing of the bowel inflammation or acquire an alternative clinical course, independent of the GI tract disorder. The systems mainly affected are the musculoskeletal system, skin, eyes, lungs and the hepatobiliary (HB) system (1). IBD-associated HB disorders typically include primary sclerosing cholangitis (PSC), autoimmune hepatitis (AIH), and less frequently, primary biliary cirrhosis (PBC), cholangiocarcinoma, nonalcoholic fatty liver disease, hepatic abscess, and hepatic vascular abnormalities (2). The activity of HB disorders is usually independent of the bowel disease and does not parallel with it. Indeed PSC, the HB disorder most frequently found in association

with IBD, can develop many years after colectomy, and IBD can appear in patients who have undergone liver transplantation for PSC (3). Concomitant IBD and PSC (IBD/PSC) are also characterized by different clinical manifestations with respect to IBD alone, suggesting that IBD/PSC may constitute a unique form of IBD (4).

Etiology of IBD-associated liver disorders

The etiology of IBD-associated HB disorders still remains unclear. AIH is commonly regarded as an autoimmune disease and shows typical features such as female predilection, presence of disease-specific autoantibodies, and responsiveness to immunosuppressive medications (5). PSC, instead, does not completely fit into the autoimmune classification and two models are classically implicated in its etiology: atypical autoimmunity and immune-mediated inflammation (6). Both IBD and its extra-intestinal manifestations are characterized by extensive infiltration of inflammatory cells, particularly lymphocytes, regardless of their localization. For example, in PSC, a massive inflammatory infiltrate is observed in hepatic portal tracts and areas of piecemeal necrosis that consists predominantly of T cells (7).

Currently, the most widely-accepted hypothesis of IBD-associated liver disease, particularly PSC, is that it occurs as a consequence of aberrant adhesion molecule expression that promotes recruitment of memory T-cells, originally activated in the gut, to the liver where they drive hepatic inflammation (8).

Specifically, expression of mucosal addressin cell adhesion molecule-1 (MAdCAM-1) and the chemokine CCL25 are normally restricted to the intestinal endothelium and small bowel epithelium, respectively, and comprise the conventional gut “postal code (9)”. In PSC, MAdCAM-1 and CCL25 are aberrantly found on portal and sinusoidal endothelium, suggesting the importance of these homing molecules for the migration of T-cells to the liver (10, 11). Together, these observations support the existence of an enterohepatic lymphocyte circulation that facilitates trafficking of T-lymphocytes from the gut to the liver that can promote liver inflammation.

Alternatively, emerging evidence suggests that T-lymphocyte priming can also occur in the liver during both homeostatic and pathologic conditions (12-14). Liver-resident antigen presenting cells (APC), such as LSEC, dendritic cells (DC), and Kupffer cells (KC), are capable of interacting with naïve T-cells and have the ability to induce regulatory T-cells (Treg) differentiation and function (15, 16). In particular, LSEC can induce both Forkhead Box Protein 3 (FoxP3) positive and negative Treg, but can also suppress CD4 and CD8 effector T-cells (14, 17-19), and are considered to be crucial for promoting T-cell tolerance within the hepatic environment.

The SAMP1/YitFc mouse model

Of the many available murine models of IBD, only few allow investigation of the earliest events associated with the onset and progression of disease.

SAMP1/YitFc mice (SAMP) represent a well-characterized model of spontaneous, chronic intestinal inflammation, whose primary disease location (*i.e.*, terminal ileum), histologic features, and response to therapy closely resemble CD, one of the idiopathic forms of IBD (20, 21). This mouse strain was derived from brother-sister breeding of wild type AKR mice and the phenotype develops spontaneously without chemical, genetic or immunological manipulation by 10 weeks of age (22). Previous unpublished findings by our group reported a liver phenotype occurring prior to the onset of intestinal inflammation in SAMP. Indeed, abundant inflammatory infiltrates were detected as early as 1-week in SAMP compared to healthy AKR controls, when no histologic evidence of ileitis is typically present (20-22). The peak of liver inflammation occurred at 4-weeks in SAMP, when ileitis is not yet detected histologically, and gradually diminished over time, most significantly in areas of lobular compared to portal involvement. Therefore liver inflammation displays an opposite tendency with respect to the ileitis, which progressively increases in severity, reaching maximum inflammation by 20-weeks. Accordingly, the SAMP model is ideal to evaluate the onset and progression of liver inflammation in the presence of chronic ileitis, and to investigate the relationship and potential mechanism(s) linking gut and liver pathologies.

Aim of the study

The presence of inflammatory infiltrates in hepatic portal tracts was previously reported in 20- to 30-week-old SAMP (21, 23); however, this observation was not further characterized. Indeed, the cellular mechanism(s) responsible for the liver phenotype observed in ileitis-prone SAMP is unknown. Interestingly, adoptive transfer of $CD4^+$ T-cells derived from SAMP gut-associated lymphoid tissue (GALT) into naïve SCID recipients results in ileitis (20), supporting a key role of $CD4^+$ T-cells in the pathogenesis of SAMP ileitis. Of note, inflammatory cells infiltrating portal tracts of PSC patients consist predominantly of T-cells, highly producing TNF (7, 24). Taken together, these findings suggest that T-cells, particularly $CD4^+$ T-cells, may be important not only in IBD, but also in its extra-intestinal manifestations, such as hepatic inflammation.

The aim of the present study is to characterize the role played by the immune compartment, particularly liver-resident $CD4^+$ T-cells, in SAMP hepatic inflammation. Herein, we hypothesize that intrahepatic $CD4^+$ T-cells undergo pathogenic activation and drive inflammation in the SAMP liver, as a consequence of impaired immunosuppression mediated by Treg.

The specific aims of this study are to:

a) Investigate the relative contribution of host intrinsic factors, *i.e.* the epithelial permeability defect characterizing SAMP, and the hematopoietic

compartment in SAMP hepatic inflammation by generating bone marrow chimeric mice and SAMPxRAG-1 KO mice

b) Test the activation phenotype and the pathogenic potential of liver- and GALT-derived $CD4^+$ T-cells from SAMP and AKR controls by flow cytometry and by adoptively transferring $CD4^+$ T-cells into naïve SCID recipient mice

c) Measure the protein expression in SAMP liver of homing molecules usually restricted to the gut that are overexpressed in PSC patients, such as MAdCAM-1 and CCL25, and the frequency of $CD4^+$ T-cells expressing their counterpart ligands, *i.e.,* α4β7 and CCR9, by flow cytometry

d) Evaluate the frequency of liver-resident tolerogenic populations, *i.e.,* LSEC and Treg, in SAMP vs. AKR by flow cytometry

e) Test the *in vitro* proliferation and suppression, respectively, of effector and regulatory $CD4^+$ T-cells resident in SAMP and AKR liver.

Materials and methods

Mice

Original AKR/J (AKR), B6.129S7-Rag1^{tm1Mom}/J (RAG-1 knockout (KO)), and C3Smn.CB17-Prkdcscid/J (SCID) mice were purchased from The Jackson Laboratory (Bar Harbor, ME). SAMP founders were provided by S. Matsumoto (Yakult Central Institute for Microbiological Research, Tokyo, Japan) (20, 22). SAMPXRAG-1 KO were generated by backcrossing RAG-1 KO onto SAMP for 10 generations. Experimental mice were maintained under specific pathogen-free conditions, fed standard laboratory chow (Harlan Teklad, Indianapolis, IN), and kept on 12h light/dark cycles. All procedures followed AALAC guidelines and were approved by CWRU's IACUC.

Histology and Immunohistochemistry

Liver and ileal tissues were processed for histology (20, 23, 25-30) and evaluated by trained pathologists (T. Roskams, J. Mize) using a novel liver and established ileal (23, 26-32) scoring systems. Immunolocalization of T-cells and TNF was performed using α-CD3 (ab5690/1:50), and α-TNF (ab1793/1:20) primary antibodies (all from Abcam, Cambridge, MA), and visualized using the Dako EnVision^{TM} System (Dako, Carpinteria, CA). Images were obtained on an Axiophot microscope and assembled by Axiovision Release 4.5 (Carl Zeiss, Inc., Thornwood, NY).

NPLC Isolation

NPLC were isolated by perfusing mice with HBSS through the hepatic portal vein, after which livers were removed and homogenized. Homogenates were incubated with agitation at 37°C for 30 min in a solution of 0.05% collagenase type IV and DNase I, in HBSS (Sigma-Aldrich, St. Louis, MO). Resulting cell suspensions were centrifuged at 300 rpm at 4°C, passed through 40-mm nylon filters, and centrifuged again at 1200 rpm at 4°C for 10 min. ACK Lysing Buffer (Invitrogen, Carlsbad, CA) was added to cell pellets for 5 min at room temperature and similarly centrifuged. Cells were washed twice and used for immediate experimentation, or further purified by centrifugation at 2500 rpm for 30 min through a 25%/50% Percoll gradient (Sigma-Aldrich), or enriched for $CD4^+$ T-cells (described below). Cells were washed twice and then used for experiments.

Flow Cytometry

Single-cell suspensions were prepared from mesenteric lymph nodes (MLN) (28) and livers, and 10^6 cells stained with the following antibodies: PerCP-labeled CD4 (RM4-5), APC-labeled CD25 (PC61) (BD Pharmingen, San Diego, CA), APC-labeled α4β7 (PS/2) (AbD Serotec, UK), PE-labeled CCR9 (242503) (R&D System, Minneapolis, MN), APC-labeled CD146 (ME-9F1), APC-Cy7-labeled CD11c (N418), PE-labeled $I\text{-}A^k$ (10-3.6), CD69 (H1.2F3), Brilliant Violet 421-labeled CD62L (MEL-14) (Biolegend, San Diego, CA), and eFluor®450-labeled

F4/80 (BM8) (eBioscience, San Diego, CA). For intracellular staining, cells were fixed after cell-surface staining, followed by permeabilization and staining with PE-labeled FoxP3 (FJK-16s) (eBioscience). Samples were analyzed with a BD FACS Calibur and CellQuest Software (Becton Dickinson, San Jose, CA).

Adoptive Transfer Model

Livers and MLN were harvested from 10- to 12-week-old donors, rendered into single cell suspensions, and purified for $CD4^+$ lymphocytes using magnetic bead separation (MACS, Miltenyi Biotec, Auburn, CA). $CD4^+$ T-cells (400,000) were transferred intraperitoneally into 6- to 8-week-old major histocompatibility complex (MHC)-matched SCIDs; untransferred SCIDs receiving PBS (vehicle) served as controls. Six-weeks post-transfer, recipient mice were euthanized and liver and ilea processed for histological evaluation and intrahepatic $CD4^+$ T-cell isolation, again using MACS (Miltenyi Biotec).

Cytokine mRNA Expression

NPLC and *ex vivo*-cultured α-CD3/CD28-activated $CD4^+$ T-cells (32) were lysed in Buffer RLT (Qiagen, Germantown, MD) immediately after collection. Total RNA was isolated using RNeasy Mini Kits (Qiagen) and reverse-transcribed to cDNA (RNA-to-cDNA kit, Applied Biosystems, Forest City, CA). Real-time qPCR was performed using the following primers: interferon (IFN-γ) (5'-GCCAAGTTTGAGGTCAACAAC-3'; 5'-CCGAATCAGCAGCGACTC-3'), tumor

necrosis factor (TNF) (5'-GCGGTGCCTATGTCTCAG-3'; 5'-GCCATTTGGGAACTTCTCATC-3'), interleukin (IL)-10 (5'-TTTAAGGGTTACTTGGGTTGC-3'; 5'-CCGCATCCTGAGGGTCTTC-3'), IL-4 (5'-GCTAGTTGTCATCCTGCTCTTC-3'; 5'-GGCGTCCCTTCTCCTGTG-3'), IL-5 (5'-GCTTCTGCACTTGAGTGTTCTG-3'; 5'-CCTCATCGTCTCATTGCTTGTC-3'), IL-13 (5'-TTGCTTGCCTTGGTGGTCTC-3'; 5'-GGGAGTCTGGTCTTGTGTGATG-3'), and β-actin (5'-CAGGGTGTGATGGGAATG-3', 5'-GTAGAAGGTGTGGTGCCAGAT-3'). RT-PCRs were performed using an Applied Biosystems Step Plus machine (Applied Biosystems). Reaction mixture consisted of 15% volume first-strand synthesis in a total volume of 20 µl that included Power SYBR Green reagents (Applied Biosystems) and 500 nM final concentrations of primers. Thermal cycling conditions were 95°C/10 min followed by 40 cycles of 95°C/15 sec and 60°C/1 min. Expression of all the genes of interest was normalized to β-actin.

Bone marrow chimeras

Reciprocal bone marrow chimeras (BMC) were generated as previously described (26), with minor modifications. Briefly, bone marrow (BM) was harvested from femurs and tibias of 4-week-old SAMP and AKR. Cell suspensions were washed and diluted to a concentration of 37.5×10^6 cells/ml in HBSS. 7.5×10^6 cells/200 µl were injected intravenously into the lateral tail veins of irradiated 10-week-old recipients. Mice were placed on antibiotic water for 2-

weeks after irradiation, then on autoclaved water for 6-weeks, after which they were euthanized, and livers and ilea collected.

MAdCAM-1 and CCL25 Protein Levels

Livers were collected and homogenized in RIPA buffer supplemented with Halt proteases and phosphate inhibitor cocktail (Pierce Biotechnology, Rockford, IL), using Lysing Matrix tubes and FastPrep®-24 (MP Biomedicals, Santa Ana, CA). Homogenates were centrifuged at 12,000 rpm, supernatants collected, and total protein content measured using BCA Protein Assay Kits (Pierce Biotechnology). After normalizing protein content, tissue homogenates were assayed for MAdCAM-1 and CCL25 protein by ELISA (R&D System).

***In vitro* T-cells proliferation and suppression assay**

Fluorescence-activated cell sorting (FACS)-purified $CD4^+$ $CD25^-$ effector T-cells (Teff) and $CD4^+$ $CD25^+$ Treg were isolated from 10-weeks-old mice. Teff were labeled with eFluor 670 (CFSE analog, 0.5 μM) and cultured with or without a 1:1 ratio of Treg. α-CD3 (1 $\mu g/ml^{-1}$) and α-CD28 (1 $\mu g/ml^{-1}$)-coated beads (Miltenyi Biotec) were added to cultures at 1:1 bead:Teff ratio. Proliferation was determined after 3 days of culture by flow cytometric dye dilution assay.

Statistical Analysis

Two-tailed unpaired Student's t-test with Welch's correction and one-way ANOVA using Bonferroni's correction were performed using GraphPad Prism 5 (GraphPad Software, Inc., La Jolla, CA). Results are expressed as mean ± SEM; p-values < 0.05 were considered significant.

Results

SAMP display immune-mediated liver inflammation

The main histopathologic features in SAMP liver consisted of portal tract inflammation characterized by T-cell infiltrates, eosinophilic polymorphonuclear lymphocytes, and macrophages, as well as focal hepatitis with T-cells infiltrating the portal-parenchymal interface (Figure 1A) with inflammatory bridging between portal tracts (Figure 1B).

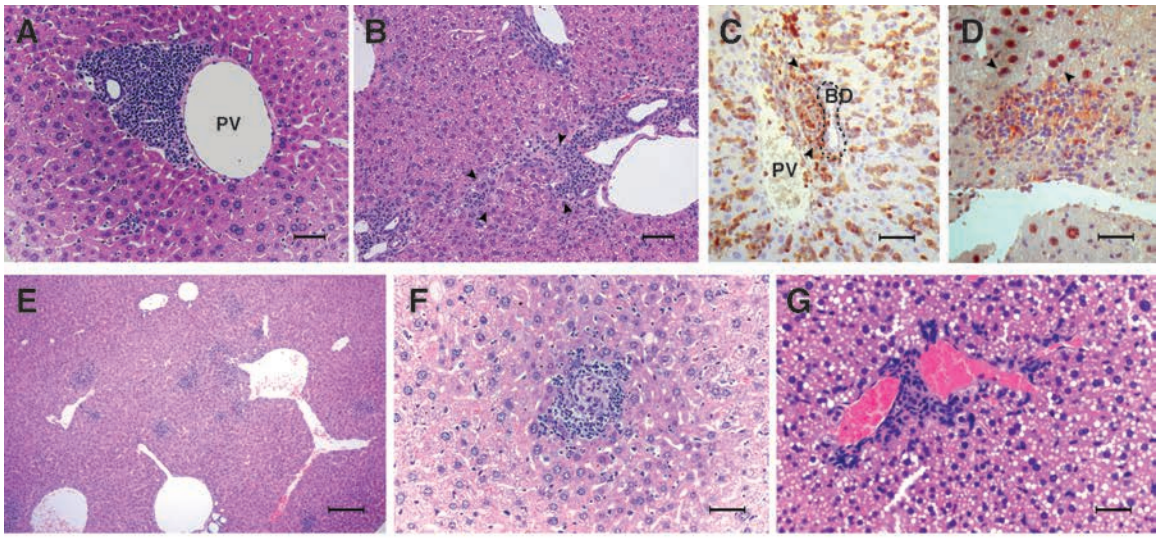

Figure 1. Liver inflammation in SAMP resembles liver involvement in IBD patients. (A) Main, pathologic features of SAMP liver include infiltration of the portal-parenchymal interface with occasional inflammatory bridging (arrows) between portal tracts (B), (C) focal $CD3^+$ T-cell infiltration (arrows) of bile duct (BD) epithelium, with TNF-expressing macrophages (arrows, D), and (E) hepatocyte anisokaryosis with inflammatory infiltration of liver lobules, often in the form of granulomas (F); in a limited number of SAMP, mild microvescicular steatosis occurs in association with sinusoidal inflammation (G). Bars: (A, B, F) 50µm, (C, D, G) 20µm, and (E) 100µm.

Remarkably, the bile duct epithelium was focally infiltrated by $CD3^+$ T-lymphocytes (Figure 1C), with TNF-expressing cells morphologically consistent with macrophages also detected in portal tracts and sinusoids (Figure 1D). In addition to prominent portal tract involvement, other pathologic features recapitulated most of those described in IBD (33), such as hepatocyte anisokaryosis (Figure 1E), granuloma-like organization of lobular inflammatory infiltrates (Figure 1F), and sinusoidal inflammation with mild microvescicular steatosis (Figure 1G). Overall, the general histopathologic findings were indicative of immune-mediated liver disease, involving both portal tracts and liver lobules, with infiltration of biliary ducts, reminiscent of the clinical phenotype of PSC/AIH overlap syndrome.

SAMP hematopoietic cells induce liver inflammation independently of host-intrinsic factors

To determine whether SAMP liver inflammation, similarly to ileitis, originates from a non-hematopoietic source (26), reciprocal BMC were generated by reconstituting irradiated SAMP with AKR BM (AKR→SAMP) and irradiated AKR with SAMP BM (SAMP→AKR). The severity of liver and ileal inflammation was assessed 8 weeks post-transplant. As previously reported (26), SAMP→AKR BMC showed no ileal inflammation (similar to AKR→AKR controls), whereas AKR→SAMP displayed inflammatory scores comparable to SAMP→SAMP BMC (Figure 2A). Conversely, liver inflammation was detected in both reciprocal BMC (SAMP→AKR and AKR→SAMP), as well as in SAMP→SAMP (Figure 2B).

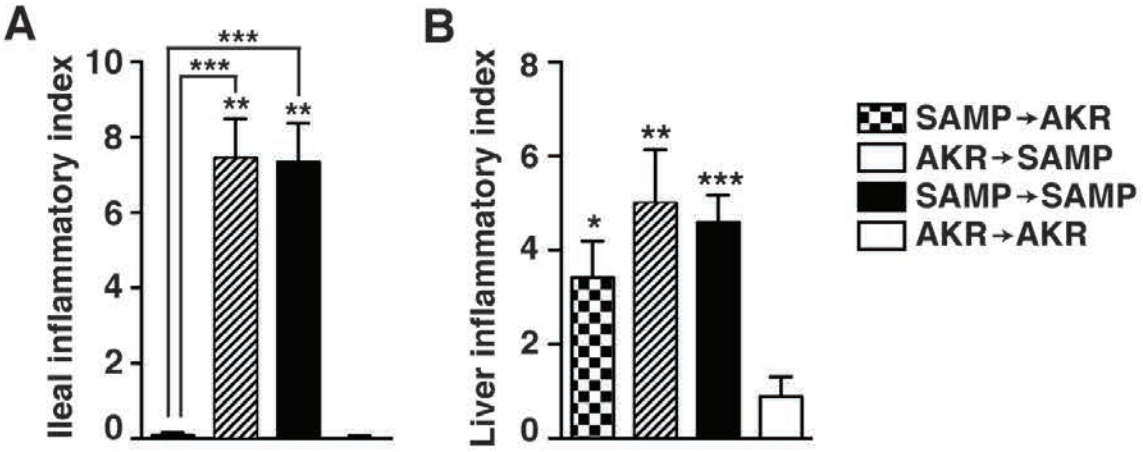

Figure 2. Hematopoietic-derived cells are required to induce SAMP liver inflammation. Liver (A) and ileal (B) diseases severity SAMP/AKR BMC (n=9-12 per group): SAMP→AKR, AKR→SAMP, SAMP→SAMP, and AKR→AKR BMC. *p<0.05, **p<0.01, ***p<0.001 vs. AKR→AKR.

Histologically, liver inflammation in AKR→SAMP, SAMP→AKR and SAMP→SAMP was similar to that observed in native SAMP and was characterized by infiltration of inflammatory cells, particularly abundant in enlarged portal tracts, with minor involvement of liver lobules (Figure 3).

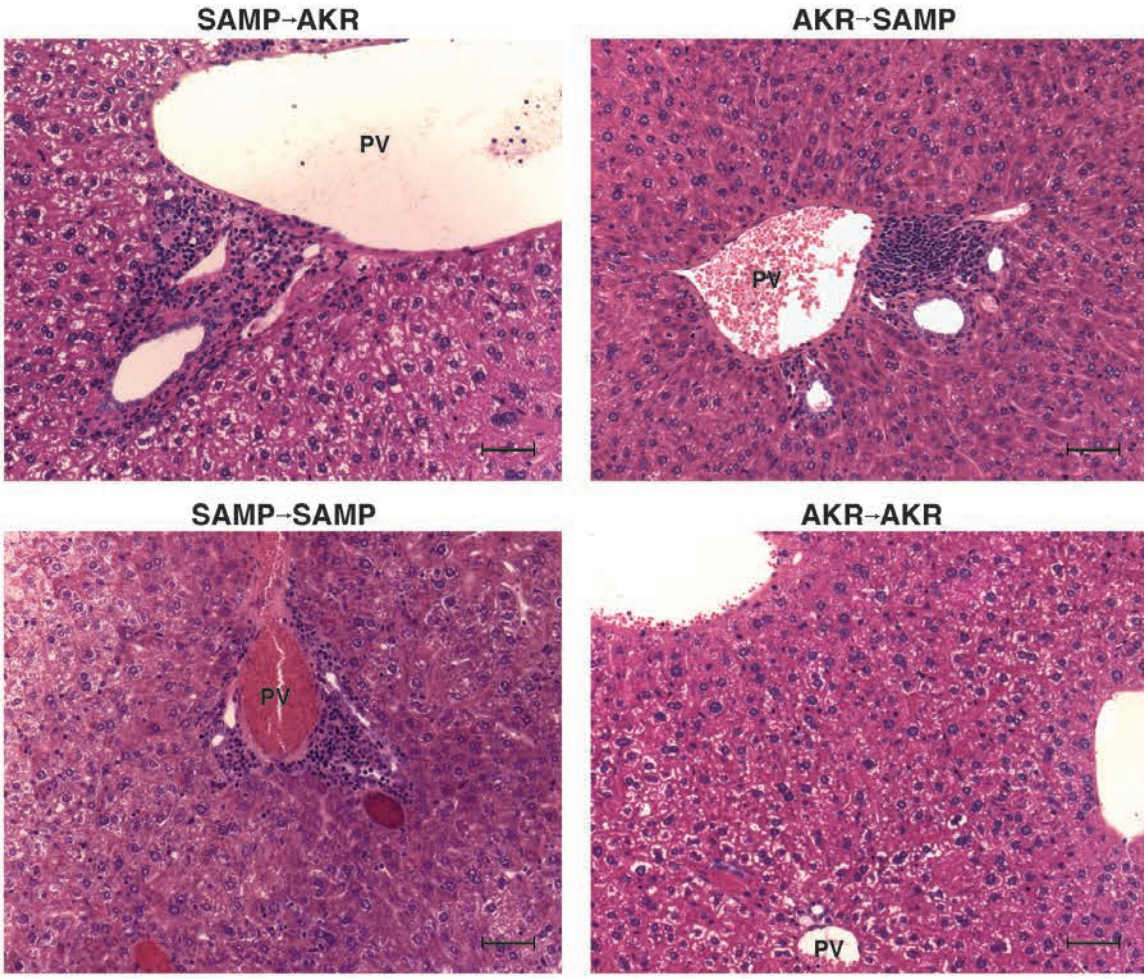

Figure 3. Hematopoietic-derived cells are required to induce SAMP liver inflammation. Representative histologic photomicrographs of SAMP/AKR BMC liver (n=9-12 per group). Bars: 70μm.

To investigate the role played by lymphocytes within the hematopoietic compartment, SAMPXRAG-1 KO mice were generated by backcrossing RAG-1-deficient mice (34) onto the SAMP background in order to produce SAMP lacking mature T- and B-lymphocytes. SAMPXRAG-1 KO mice developed only mild, if any, liver inflammation compared to SAMPXRAG-1 wild-type (WT) littermates (Figure 4).

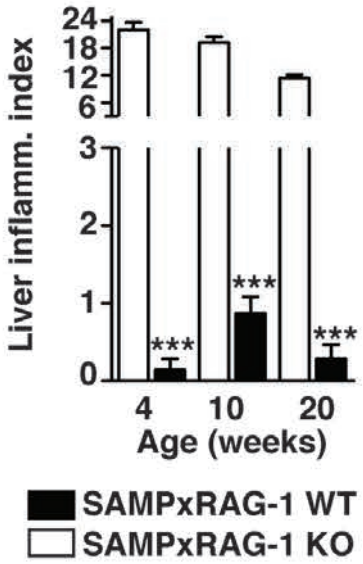

Figure 4. Liver inflammation is abrogated in the absence of mature lymphocytes in SAMP. Severity of liver inflammation in SAMPXRAG-1 KO vs. WT mice (n=7-14 per group). ***p<0.001 vs. SAMPxRAG-1 WT.

Interestingly, cytokine gene expression measured during peak liver inflammation in SAMP (4 weeks of age) showed increased IL-1β, IFNγ, and TNF mRNA transcript levels and decreased IL-4, IL-13 and IL-10, compared to age-matched AKR (Figure 5), indicating that the cytokine milieu during peak hepatic inflammation is skewed towards a proinflammatory/Th1 profile.

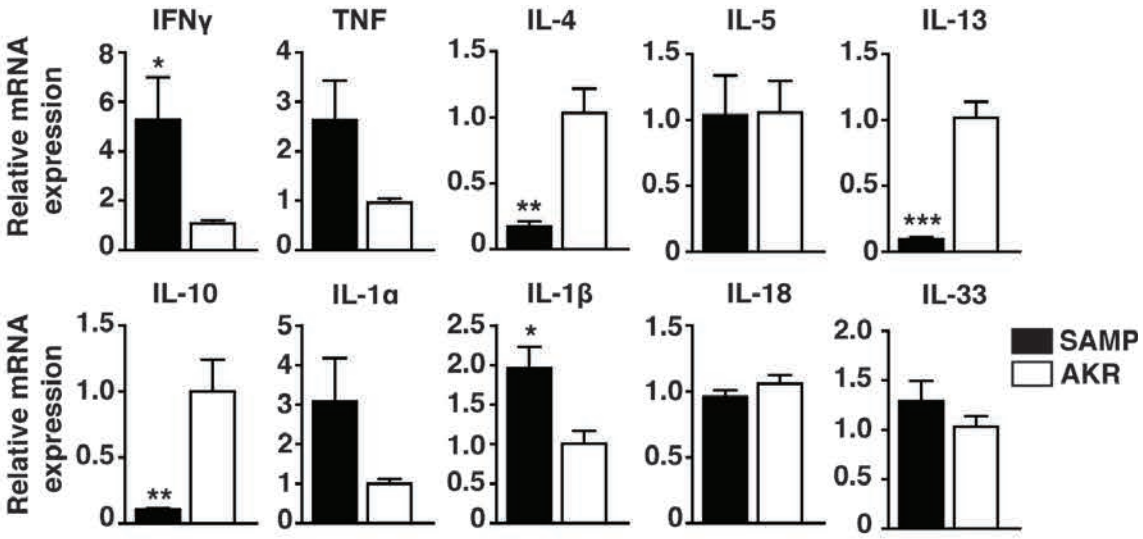

Figure 5. Non-parenchymal liver cells overproduce Th1-like cytokines in inflamed SAMP liver. Relative mRNA expression of hepatic proinflammatory, Th1, and Th2 cytokines in NPLC from 4 weeks old mice (n=8). *p<0.05, **p<0.01 vs. AKR.

Previous findings from our group highlighted a marked increase of $CD3^+$ T-cells, specifically of $CD4^+$ T-cells, as early as 4 weeks of age, while no difference in the percentages of $CD8^+$ T-cells was observed between SAMP and AKR livers (unpublished data). Moreover, $CD4^+$ T-cell expressed CD69, $CD44^{hi}$ and CD62L at higher percentages in SAMP vs. AKR liver (unpublished data), indicating an increased pool of activated effector and naïve liver T-cells that retain the ability to recirculate through lymph nodes.

SAMP intrahepatic CD4$^+$ T-cells transfer both liver and ileal inflammation into SCID recipient mice

Interestingly, at 10-12 weeks, when both ileal and liver inflammation are established, a distinct population of CD4$^+$CD62L$^+$CD69$^+$ T-cells was identified in SAMP MLN that was substantially diminished in the liver (Figure 6).

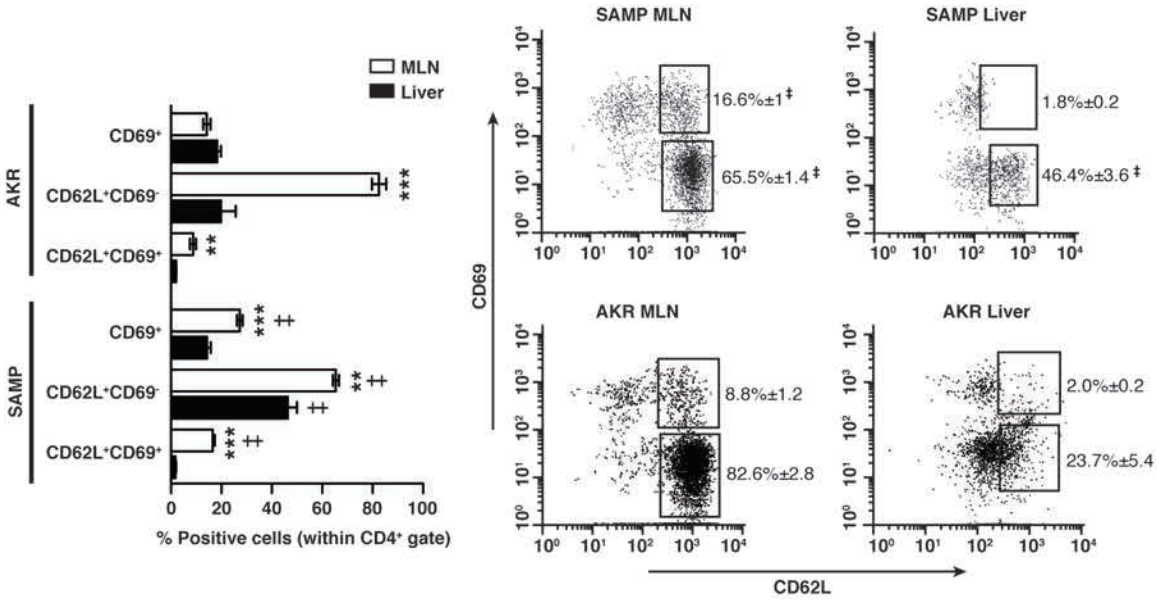

Figure 6. Phenotypic activation of MLN- and liver-derived CD4$^+$ T-cells. Percentages of activated CD4$^+$ T-cell subsets (left) and representative flow cytometry analysis (right) in 10-12-wk-old mice (n=3-5). **p<0.01, ***p<0.001, ‡p<.01 vs. AKR.

These cells likely represent a pathogenic population comprised of naïve T-cells that have homed to the MLN and are undergoing activation after exposure to a Th1-polarizing environment. Indeed, GALT-derived CD4$^+$ T-cells from SAMP have been shown to induce ileitis when adoptively transferred into immunodeficient recipients (20, 27, 29, 35). Contrary to that previously reported

in 4 weeks old livers, the percentages of $CD4^+CD69^+$ T-cells were not increased in older (10-12 weeks) SAMP vs. AKR (Figure 6), confirming that SAMP liver attains an active state of inflammation early, and sustains severe disease until 10 weeks, when inflammation begins to diminish.

We next determined whether $CD4^+$ effector T-cells derived from SAMP liver had the ability to transfer either liver and/or ileal disease. Liver inflammation developed following adoptive transfer of liver-derived $CD4^+$ T-cells from SAMP (Figure 7), while MLN-derived cells were not able to induce significant liver inflammation vs. AKR donor T-cells (Figure 8).

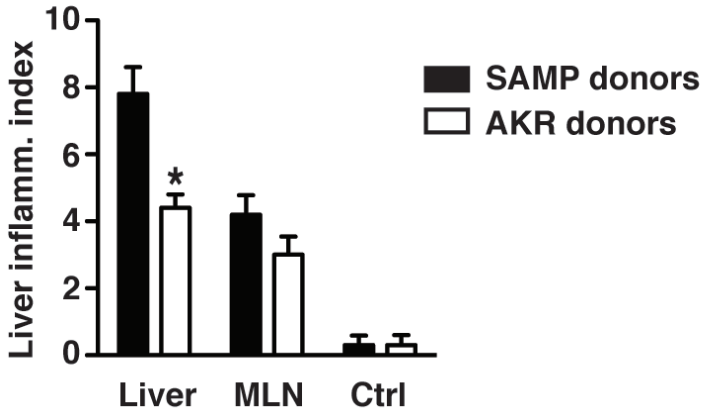

Figure 7. Liver-derived SAMP $CD4^+$ T-cells are uniquely able to induce hepatic inflammation in SCID recipients. Liver inflammation in recipient mice following adoptive transfer of donor $CD4^+$ T-cells derived from liver or MLN of donor mice; recipients receiving vehicle only served as controls (Ctrl) (n=8-10). *$p<0.05$ vs. AKR donors.

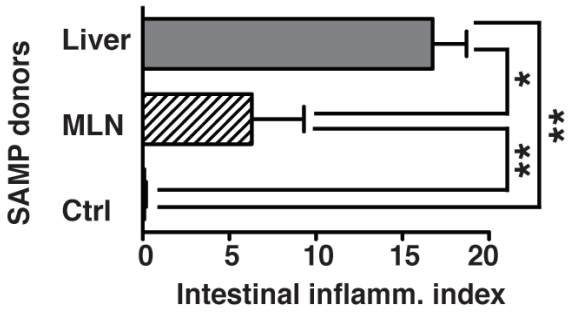

Figure 8. Intrahepatic SAMP CD4$^+$ T-cells can transfer both hepatic and ileal inflammation whereas MLN-derived CD4$^+$ T-cells transfer only ileitis. Ileitis severity in SCID mice receiving SAMP CD4$^+$ T-cells derived from MLN or liver of donor mice. *p<0.05, **p<0.01, ***p<0.001.

Similar to native SAMP (Figure 5), intrahepatic CD4$^+$ T-cells from SCIDs receiving SAMP liver cells expressed higher levels of TNF and IFNγ mRNA transcripts compared to those receiving MLN T-cells (Figure 9).

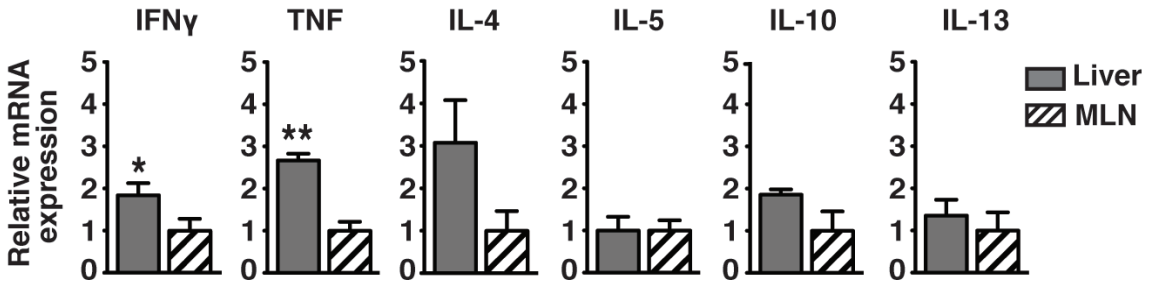

Figure 9. Intrahepatic CD4$^+$ T-cells from SCID receiving SAMP donor cells overexpress Th1 cytokines. Th1/Th2 cytokine mRNA expression in activated *ex vivo*-cultured intrahepatic CD4$^+$ T-cells from recipients of donor SAMP liver vs. MLN cells (N=4 per group). *p<0.05, **p<0.01

Importantly, prominent ileitis developed in recipient mice following transfer of liver-derived SAMP CD4$^+$ T-cells that was more severe than observed after transfer of MLN-derived cells, as well as control (untransferred) recipients, which displayed no histologic signs of inflammation (Figure 8 and 10).

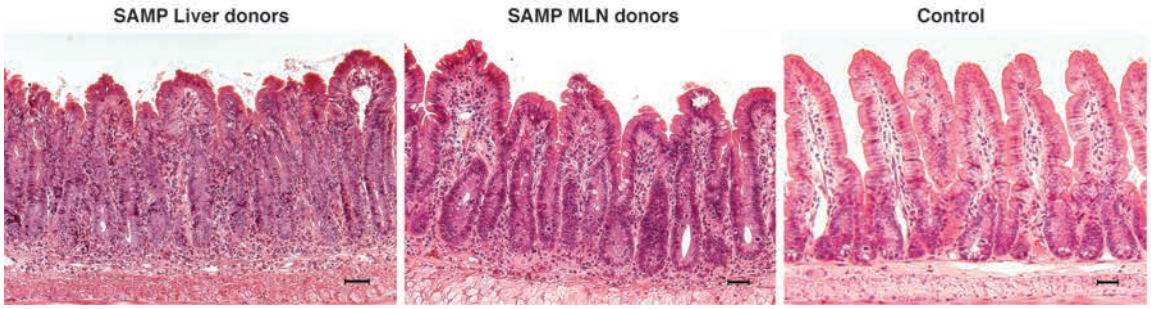

Figure 10. Liver-derived SAMP CD4$^+$ T-cells induce more severe ileitis respect to MLN-derived SAMP CD4$^+$ T-cells. Representative histologic photomicrographs displaying epithelial crypt hypertrophy and elongation, and villous blunting with dense inflammatory infiltrates throughout mucosa and submucosa in recipients of liver-derived donor cells (left), which was less severe in ilea adoptively transferred with MLN-derived donor cells (middle) and Ctrl (right). Bars: 50μm.

Together, these data suggest that liver-derived effector CD4$^+$ T-cells have the ability to drive both liver and ileal inflammation in native SAMP, while those derived from GALT (*i.e.*, MLN) can only produce ileitis.

Gut-specific homing molecules are unchanged in SAMP liver

According to the most commonly-accepted hypothesis, IBD-associated liver inflammation is the result of lymphocyte homing, specifically of $\alpha_4\beta_7^+$ and/or CCR9$^+$ cells that are originally activated in the gut and are subsequently recruited to the liver (8). Interestingly, the percentages of CD4$^+$ T-cells positive or highly-expressing the homing receptors, $\alpha_4\beta_7$ and CCR9, were unchanged in SAMP vs. AKR livers during peak inflammation (Figure 11).

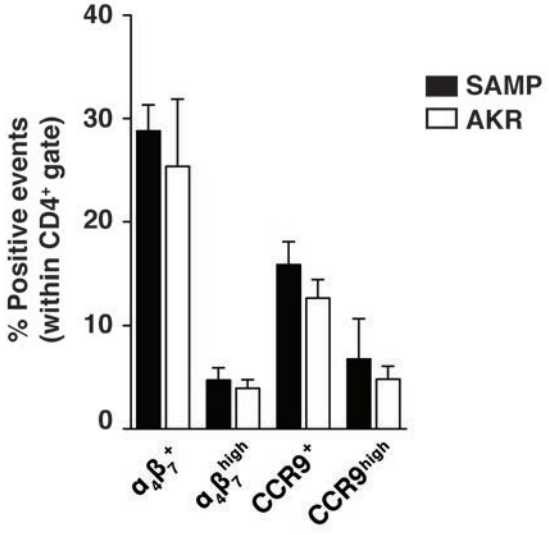

Figure 11. CD4$^+$ T-cells do not overexpress $\alpha_4\beta_7^+$ and CCR9$^+$ in SAMP liver. (A) Percentages of intrahepatic CD4$^+$ T-cell subsets from 4 weeks old mice. Isolated NPLC were first gated on CD4 and successively on $\alpha_4\beta_7$ and CCR9, distinguishing between overall positive cells and highly expressing cells (n=5).

Consistently, protein levels of MAdCAM-1 and CCL25, cognate ligands for $\alpha_4\beta_7$ and CCR9, were also similar in SAMP vs. AKR livers at 4 weeks, and decreased or did not change, respectively, at 20 weeks (Figure 12).

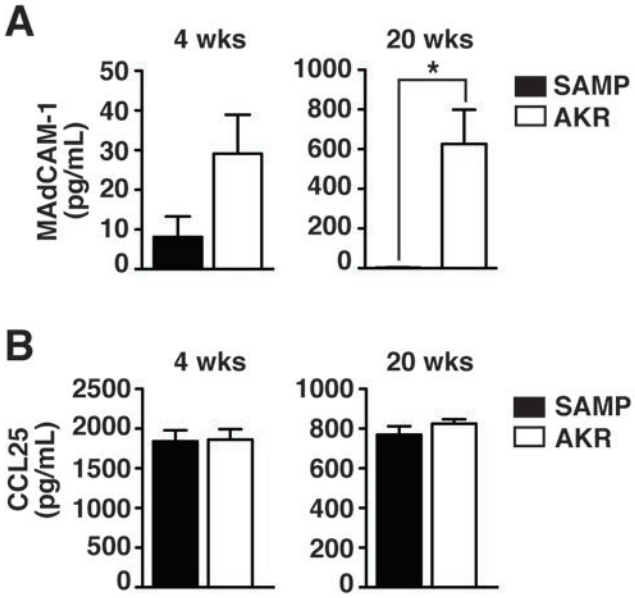

Figure 12. MAdCAM-1 and CCL25 expression is not increased in SAMP liver. Protein concentration of MAdCAM-1 (A) and CCL25 (B) measured by ELISA in liver homogenates of 4 and 20 weeks old mice; *p<0.05.

These data suggest that SAMP are not likely experiencing enhanced recruitment of gut-activated $CD4^+$ T-cells to the liver.

LSEC and Treg frequencies are altered in SAMP liver

To test whether the pathogenic potential of SAMP liver effector $CD4^+$ T-cells may be due to altered antigen presentation by liver-resident APC, the frequency of APC subsets and their expression of MHC class II $I\text{-}A^k$ were measured. Surprisingly, no differences were observed in the frequency of either $F4/80^+$ macrophages or $CD11c^+$ DC between SAMP and AKR livers, while $CD146^+$ LSEC were markedly decreased and displayed increased $I\text{-}A^k$ expression in SAMP compared to AKR during peak liver inflammation (Figure 14 and 15).

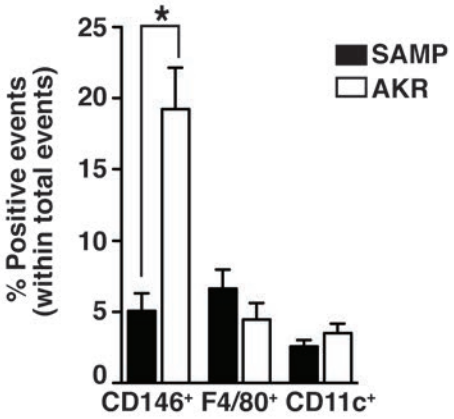

Figure 14. LSEC frequency is decreased in SAMP liver. Percentages of intrahepatic positive cells for F4/80, CD11c, CD146 in total cell gate; one observation (n) represents pooled samples from 2-3 mice/livers; (n=4-6); *p<0.05

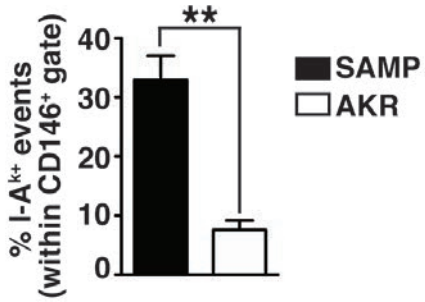

Figure 15. LSEC overexpress MHC class II $I\text{-}A^{k+}$ in SAMP liver. Percentages of intrahepatic positive cells for IA^k in CD146 gate; one observation (n) represents pooled samples from 2-3 mice/livers; (n=4-6), **p<0.001.

The reduced frequency of LSEC in SAMP also associated with a decreased percentage of hepatic FoxP3^{+} Treg (Figure 16).

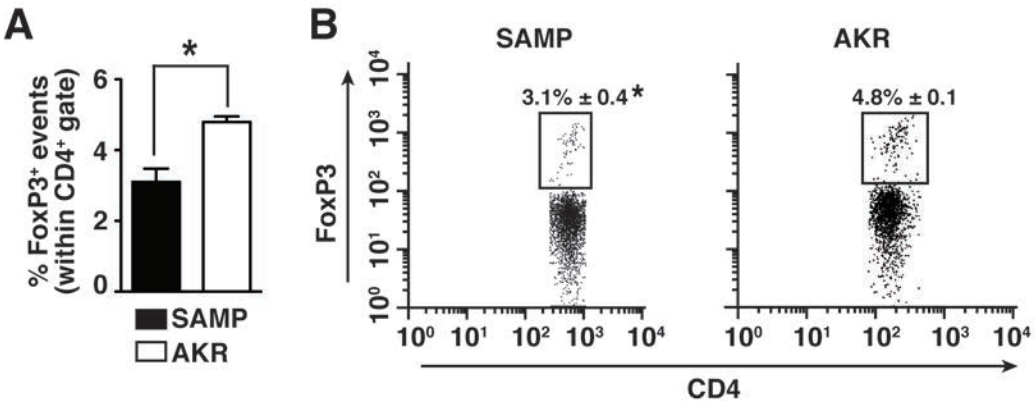

Figure 16. FoxP3^{+} Treg frequency is decreased in SAMP liver. (A) Percentages of intrahepatic FoxP3^{+} cells calculated within CD4 gate, with (B) representative plots (n=3), *p<0.05.

Together, these data suggest that LSEC-mediated induction of hepatic Treg may be impaired in SAMP, which can promote immunoregulatory dysfunction and local inflammation within the liver.

In vitro immunosuppression by Treg is impaired in SAMP liver

To investigate whether the immunosuppressive function of liver-resident Treg is altered in SAMP liver, we used the CFSE suppression assay to evaluate both the proliferation of effector CD4^{+} T-cells and the suppression of Treg. Effector CD4^{+} CD25^{-} T-cells and CD4^{+} CD25^{+} Treg were isolated by FACS from SAMP and AKR livers according to the gating strategy showed in Figure 17.

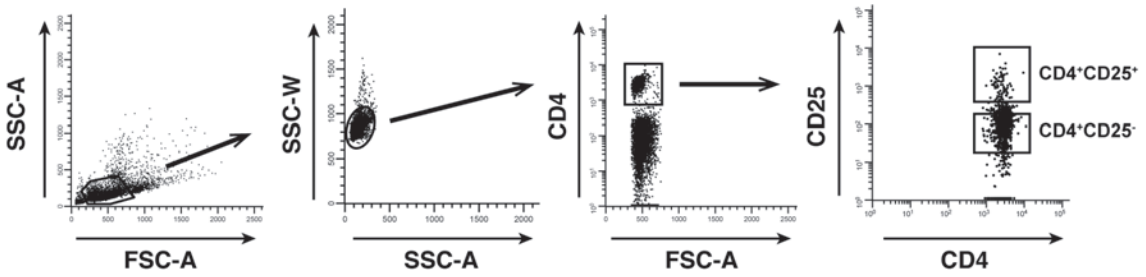

Figure 17. FACS sorting scheme for isolation of $CD4^+CD25^+$ and $CD4^+CD25^-$ cells. $CD4^+CD25^+$ and $CD4^+CD25^-$ cells were isolated from SAMP and AKR mice by FACS. Figure shows sequential gating on lymphocytes by FSC-A and SSC-A, followed by exclusion of aggregates by SSC-W and SSC-A. Singlet lymphocytes were selected on CD4 positive fluorescence and then CD25 positive and negative expression.

Effector T-cells were labeled with eFluor 670 (CFSE analog) and cultured with α-CD3/CD28, with or without Treg for 3 days. We found that the percentage of dividing cells (reduced CFSE) stimulated with α-CD3/CD28 was higher in SAMP compared to AKR cultures (87.1% vs. 77.4%, respectively) (Figure 18), suggesting that effector $CD4^+$ T-cells over-proliferate in SAMP inflamed liver compared to AKR controls.

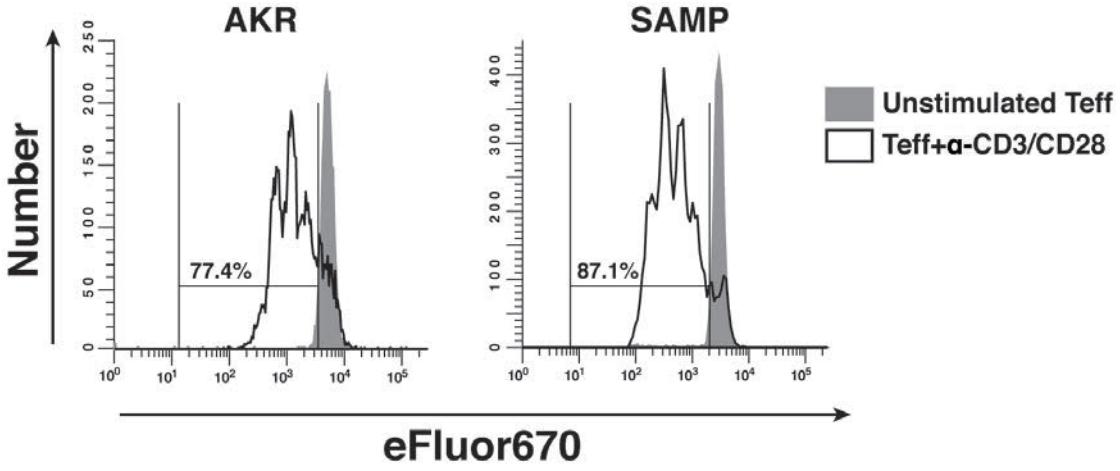

Figure 18. Effector $CD4^+$ T-cells display increased proliferation *in vitro* in SAMP liver. $CD4^+$ $CD25^-$ cells (Teff) were isolated from 10-week-old SAMP and AKR mice by FACS, labeled with eFluor670 dye and cultured *in vitro* in the presence or absence of α-CD3/CD28 for 3 days. Histograms show the proliferation of viable, CD4-gated cells in the absence (gray peaks) and presence (white peaks) of α-CD3/CD28. Percentages are referred to dividing cells in the presence of α-CD3/CD28 (n=15 pooled mice per group).

Suppression by Treg is expressed as the percentage of proliferating cells (eFluor 670 ‘‘low’’) inhibited by co-culture with Tregs, and was calculated by normalizing the difference of proliferating cells with and without Treg to the proliferation in the absence of Treg. Interestingly, liver-resident Treg from SAMP were less effective at suppressing the proliferation of hepatic effector $CD4^+$ T-cells than Treg from AKR (5.3% vs. 18.3%, respectively) (Figure 19).

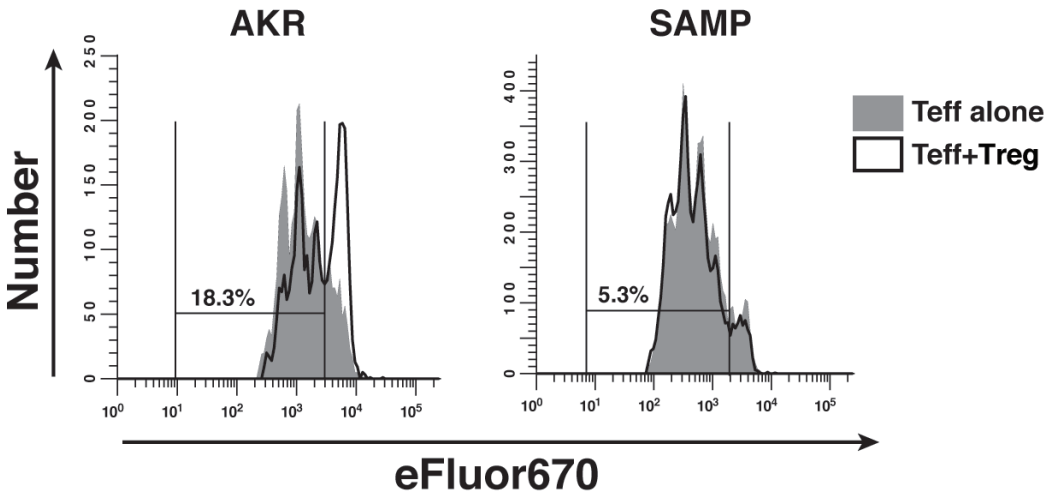

Figure 19. Treg are dysfunctional *in vitro* in SAMP liver. $CD4^+$ $CD25^-$ (Teff) and $CD4^+$ $CD25^+$ (Treg) cells were isolated from 10-week-old SAMP and AKR mice by FACS. Teff were labeled with eFluor670 dye and cultured *in vitro* in the presence of α-CD3/CD28 with or without Treg for 3 days. Histograms show the proliferation of viable, CD4-gated cells in the absence (gray peaks) and presence (white peaks) of Treg (B). Percentages are referred to Treg suppression (n=15 pooled mice per group).

These data demonstrate that liver-resident Treg from SAMP are dysfunctional *in vitro* and unable to suppress the proliferation of hepatic effector $CD4^+$ T-cells as effectively as Treg from AKR control.

Discussion

Although liver disease has previously been reported in ileitis-prone SAMP mice (22, 23), the precise histologic features, onset and progression of disease, pathogenic mechanism(s), as well as its translational implications to IBD, have not been fully addressed. Interestingly, evaluation of SAMP livers suggests a clinical phenotype resembling PSC/AIH overlap syndrome, which can also represent a comorbidity with IBD (33). PSC/AIH overlap syndrome is defined as an immune-mediated disorder with cholangiographic findings, and histologic, biologic and/or clinical features of AIH. Histologic characteristics of AIH include piecemeal necrosis, lymphocyte rosetting, and moderate to severe periportal or periseptal inflammation (36), which are features also found in SAMP livers.

Although liver involvement in IBD is commonly regarded as a consequential secondary event to gut inflammation, peak hepatic inflammation occurs in SAMP as early as 4 weeks of age, prior to the onset of ileitis. This finding suggests that in SAMP, the presence of an inflamed gut is not required to trigger hepatic inflammation and that other mechanism(s), intrinsic to the liver or host, may induce liver disease. It could also be postulated that the inherent epithelial barrier defect present in SAMP ileum (26) facilitates translocation of luminal antigens into the immune-tolerant gut, and subsequently into the liver, increasing local antigen encounter. In this scenario, the liver could be prone to early challenge and generate a vigorous inflammatory response induced by mechanism(s) involving the loss of hepatic tolerance. However, we show that SAMP

hematopoietic cells are uniquely able to induce liver, but not ileal, inflammation in AKR recipients independently of SAMP-inherent factors, such as the ileal permeability defect. Therefore, unlike ileitis in SAMP mice, the 'leaky gut' may facilitate, but does not appear to be the primary mechanism leading to, liver disease. Additional defects in the immune compartment are likely required to induce the hepatic phenotype. Nonetheless, irradiated SAMP receiving AKR BM also displayed hepatic inflammation, even in the presence of a healthy immune compartment, a finding that may be due to pathogenic interaction(s) of healthy AKR immune cells with the diseased SAMP host, which survive irradiation. Aberrantly activated AKR immune cells can then enter the enterohepatic circulation and contribute to both organ phenotypes. In fact, gut- and liver-activated lymphocytes have been shown to migrate to the liver and gut, respectively, particularly $CD8^+$ T-cells in the former, and $CD4^+$ T-cells in the latter, case (37, 38).

The concept of a pivotal role for the immune compartment, particularly lymphocytes, during SAMP liver inflammation is further supported by the hepatic phenotype observed in SAMPXRAG-1 KO mice, wherein the absence of mature lymphocytes is sufficient to abrogate liver disease, even in the presence of a compromised intestinal barrier. Functional lymphocytes are therefore necessary for the development of SAMP liver disease, and similar to the early inductive phase of ileitis wherein Th1 cytokines predominate (20), the SAMP hepatic environment is also Th1-skewed and enriched for $CD4^+$ T-cells. This Th1 milieu is already established at 4 weeks, before ileitis, and suggests the presence of a

shared pathogenic mechanism between the two organs that is able to induce similar phenotypes and immune responses, albeit temporally separated.

Interestingly, SAMP-derived intrahepatic $CD4^+$ T-cells display an activated phenotype and are able to adoptively transfer both liver and ileal inflammation, while GALT-derived $CD4^+$ T-cells transfer ileitis only. Therefore the liver, rather than the gut, provides a pool of pathogenic Th1 $CD4^+$ T-cells able to induce hepatic inflammation. This contrasts with the widely accepted hypothesis that IBD-associated liver inflammation is mediated by long-lived, GALT-derived $a4b7^+$ and $CCR9^+$ T-lymphocytes later recruited to the liver (11, 39, 40). Unlike the ileal phenotype (23, 30, 31, 41), we were unable to detect any significant differences in intrahepatic $a4b7^+$ and $CCR9^+$ $CD4^+$ T-cell frequencies or their corresponding ligands, MAdCAM-1 and CCL25, respectively, in SAMP compared to AKR livers. This provides further strength for the hypothesis that host hepatic defects, rather than aberrant recruitment of gut-activated lymphocytes, are responsible for the ileitis-associated liver phenotype observed in SAMP mice. Recently, LSEC have been reported to induce expression of a4b7 and CCR9 in naïve $CD4^+$ lymphocytes (38), challenging the concept that lymphocytes expressing these molecules are exclusively gut-derived, and suggests instead that priming of gut tropic $CD4^+$ T-cells may also occur in the liver. This implies that aberrant expression of MAdCAM-1 and CCL25 reported in PSC patients (10, 11), may not be the only cause of increased intrahepatic lymphocyte frequency observed in IBD-associated liver inflammation.

Effector functions of intrahepatic T-lymphocytes depend both on their site of primary activation and on the type of T-cells considered, particularly whether these are $CD4^+$ or $CD8^+$ T-lymphocytes (12, 42). Increasing evidence suggests that antigen presentation in the liver mainly results in activation of $CD8^+$ T-cells, whereas the effect on $CD4^+$ lymphocytes is still controversial (13, 14, 43). Despite the pro-inflammatory environment characteristic of the SAMP liver during peak inflammation, we could not detect significant differences in DC and KC frequencies and their MHC class II expression between SAMP and AKR. Therefore, increased antigen presentation by traditional liver-resident APC is unlikely to be the main mechanism by which $CD4^+$ T-cells acquire pathogenic potential in the inflamed SAMP liver. Typically, antigen presentation by LSEC to $CD4^+$ T-cells does not result in an effective immune response, but rather leads to the induction of hepatic tolerance (14, 43). LSEC-mediated tolerance can be conferred to $CD4^+$ T-cells by several mechanisms, and relevant to this study, by induction of $CD4^+$ $FoxP3^+$ Treg, but also by direct inhibition of Th1 effector $CD4^+$ cells (17, 18). LSEC normally express low levels of MHC class II as a consequence of exposure to IL-10, abundant in the homeostatic liver, which determines a shift from an activated to inhibitory phenotype with the ability to suppress IFN-γ secretion from $CD4^+$ T-cells (17, 44). LSEC are not only decreased in frequency in inflamed SAMP liver, but also display greater expression of MHC class II, consistent with diminished IL-10 mRNA expression observed in SAMP NPLC. As such, downregulation of IL-10 in inflamed SAMP liver likely determines a shift in LSEC phenotype and function, impairing their

ability to effectively suppress effector $CD4^+$ T-cells. Along with reduced LSEC, we observed diminished $FoxP3^+$ Treg in SAMP liver, which suggests that the decreased frequency of LSEC and of anti-inflammatory signals may deter the generation of homeostatic hepatic $FoxP3^+$ Treg. Accordingly, it is possible that liver inflammation in SAMP mice does not originate from an inciting intestinal event, but from (an) inherent host defect(s). Indeed, GALT-derived SAMP Treg are unable to suppress *in vivo* effector $CD4^+$ T-cell proliferation and display a pro-inflammatory phenotype (45). In this scenario, the reduced frequency and suppressive capacity of hepatic Treg would allow the uncontrolled proliferation of pathogenic Th1-activated intrahepatic $CD4^+$ T-cells and drive liver inflammation in SAMP. Given the ability of intrahepatic $CD4^+$ T-cells to also transfer ileal inflammation into immunodeficient recipient mice, it is likely that their uncontrolled proliferation may also contribute to SAMP ileitis.

Conclusions

In the present study, we identify one of the possible mechanisms contributing to IBD-associated liver disease in the ileitis-prone SAMP model and raise the possibility that hepatic involvement is more than a mere extra-intestinal manifestation of IBD. Overall, these results support a pathogenic role of intrahepatic $CD4^+$ T-cells in both SAMP liver and intestinal inflammation, and suggest that impaired hepatic regulatory pathways may be responsible for their acquired pathogenicity and function. Moreover, these findings suggest that liver and intestinal inflammation in IBD, or at least in a subset of patients, may develop as concomitant disease processes, based on common host-driven immune defects.

Acknowledgments

I would like to acknowledge Theresa T. Pizarro and Massimo Pinzani for designing and supervising this study, obtaining funding, and their critical revision of this manuscript; Giacomo Laffi, Fabio Cominelli and Alex Y. Huang for material support and their important intellectual contribution. I also acknowledge Marco Brogi, Wendy A. Goodman, Saada Eid, Carlo De Salvo and Xiao-Ming Wang that contributed to this study with their technical support and expertise.

References

1. Trikudanathan G, Venkatesh PG, Navaneethan U. Diagnosis and therapeutic management of extra-intestinal manifestations of inflammatory bowel disease. Drugs 2012;72:2333-2349.

2. Lichtenstein DR. Hepatobiliary complications of inflammatory bowel disease. Curr Gastroenterol Rep 2011;13:495-505.

3. Jorgensen KK, Lindstrom L, Cvancarova M, Karlsen TH, Castedal M, Friman S, Schrumpf E, et al. Immunosuppression after liver transplantation for primary sclerosing cholangitis influences activity of inflammatory bowel disease. Clin Gastroenterol Hepatol 2013;11:517-523.

4. Loftus EV, Jr., Harewood GC, Loftus CG, Tremaine WJ, Harmsen WS, Zinsmeister AR, Jewell DA, et al. PSC-IBD: a unique form of inflammatory bowel disease associated with primary sclerosing cholangitis. Gut 2005;54:91-96.

5. Heneghan MA, Yeoman AD, Verma S, Smith AD, Longhi MS. Autoimmune hepatitis. Lancet 2013;382:1433-1444.

6. Eaton JE, Talwalkar JA, Lazaridis KN, Gores GJ, Lindor KD. Pathogenesis of primary sclerosing cholangitis and advances in diagnosis and management. Gastroenterology 2013;145:521-536.

7. Hashimoto E, Lindor KD, Homburger HA, Dickson ER, Czaja AJ, Wiesner RH, Ludwig J. Immunohistochemical characterization of hepatic lymphocytes in primary biliary cirrhosis in comparison with primary sclerosing cholangitis and autoimmune chronic active hepatitis. Mayo Clin Proc 1993;68:1049-1055.

8. Adams DH, Eksteen B, Curbishley SM. Immunology of the gut and liver: a love/hate relationship. Gut 2008;57:838-848.

9. Tufail S, Badrealam KF, Sherwani A, Gupta UD, Owais M. Tissue specific heterogeneity in effector immune cell response. Front Immunol 2013;4:254.

10. Grant AJ, Lalor PF, Hubscher SG, Briskin M, Adams DH. MAdCAM-1 expressed in chronic inflammatory liver disease supports mucosal lymphocyte adhesion to hepatic endothelium (MAdCAM-1 in chronic inflammatory liver disease). Hepatology 2001;33:1065-1072.

11. Eksteen B, Grant AJ, Miles A, Curbishley SM, Lalor PF, Hubscher SG, Briskin M, et al. Hepatic endothelial CCL25 mediates the recruitment of CCR9+ gut-homing lymphocytes to the liver in primary sclerosing cholangitis. J Exp Med 2004;200:1511-1517.

12. Derkow K, Loddenkemper C, Mintern J, Kruse N, Klugewitz K, Berg T, Wiedenmann B, et al. Differential priming of CD8 and CD4 T-cells in animal models of autoimmune hepatitis and cholangitis. Hepatology 2007;46:1155-1165.

13. Bertolino P, Bowen DG, McCaughan GW, Fazekas de St Groth B. Antigen-specific primary activation of CD8+ T cells within the liver. J Immunol 2001;166:5430-5438.

14. Kruse N, Neumann K, Schrage A, Derkow K, Schott E, Erben U, Kuhl A, et al. Priming of CD4+ T cells by liver sinusoidal endothelial cells induces CD25low forkhead box protein 3- regulatory T cells suppressing autoimmune hepatitis. Hepatology 2009;50:1904-1913.

15. Thomson AW, Knolle PA. Antigen-presenting cell function in the tolerogenic liver environment. Nat Rev Immunol 2010;10:753-766.

16. Racanelli V, Rehermann B. The liver as an immunological organ. Hepatology 2006;43:S54-62.

17. Carambia A, Frenzel C, Bruns OT, Schwinge D, Reimer R, Hohenberg H, Huber S, et al. Inhibition of inflammatory CD4 T cell activity by murine liver sinusoidal endothelial cells. J Hepatol 2013;58:112-118.

18. Carambia A, Freund B, Schwinge D, Heine M, Laschtowitz A, Huber S, Wraith DC, et al. TGF-beta-dependent induction of CD4(+)CD25(+)Foxp3(+) Tregs by liver sinusoidal endothelial cells. J Hepatol 2014;61:594-599.

19. Schildberg FA, Hegenbarth SI, Schumak B, Scholz K, Limmer A, Knolle PA. Liver sinusoidal endothelial cells veto CD8 T cell activation by antigen-presenting dendritic cells. Eur J Immunol 2008;38:957-967.

20. Kosiewicz MM, Nast CC, Krishnan A, Rivera-Nieves J, Moskaluk CA, Matsumoto S, Kozaiwa K, et al. Th1-type responses mediate spontaneous ileitis in a novel murine model of Crohn's disease. J Clin Invest 2001;107:695-702.

21. Pizarro TT, Pastorelli L, Bamias G, Garg RR, Reuter BK, Mercado JR, Chieppa M, et al. SAMP1/YitFc mouse strain: a spontaneous model of Crohn's disease-like ileitis. Inflamm Bowel Dis 2011;17:2566-2584.

22. Matsumoto S, Okabe Y, Setoyama H, Takayama K, Ohtsuka J, Funahashi H, Imaoka A, et al. Inflammatory bowel disease-like enteritis and caecitis in a senescence accelerated mouse P1/Yit strain. Gut 1998;43:71-78.

23. Rivera-Nieves J, Ho J, Bamias G, Ivashkina N, Ley K, Oppermann M, Cominelli F. Antibody blockade of CCL25/CCR9 ameliorates early but not late chronic murine ileitis. Gastroenterology 2006;131:1518-1529.

24. Bo X, Broome U, Remberger M, Sumitran-Holgersson S. Tumour necrosis factor alpha impairs function of liver derived T lymphocytes and natural killer cells in patients with primary sclerosing cholangitis. Gut 2001;49:131-141.

25. Reuter BK, Pastorelli L, Brogi M, Garg RR, McBride JA, Rowlett RM, Arrieta MC, et al. Spontaneous, immune-mediated gastric inflammation in SAMP1/YitFc mice, a model of Crohn's-like gastritis. Gastroenterology 2011;141:1709-1719.

26. Olson TS, Reuter BK, Scott KG, Morris MA, Wang XM, Hancock LN, Burcin TL, et al. The primary defect in experimental ileitis originates from a nonhematopoietic source. J Exp Med 2006;203:541-552.

27. Bamias G, Martin C, Mishina M, Ross WG, Rivera-Nieves J, Marini M, Cominelli F. Proinflammatory effects of TH2 cytokines in a murine model of chronic small intestinal inflammation. Gastroenterology 2005;128:654-666.

28. Bamias G, Okazawa A, Rivera-Nieves J, Arseneau KO, De La Rue SA, Pizarro TT, Cominelli F. Commensal bacteria exacerbate intestinal inflammation but are not essential for the development of murine ileitis. J Immunol 2007;178:1809-1818.

29. Olson TS, Bamias G, Naganuma M, Rivera-Nieves J, Burcin TL, Ross W, Morris MA, et al. Expanded B cell population blocks regulatory T cells and exacerbates ileitis in a murine model of Crohn disease. J Clin Invest 2004;114:389-398.

30. Rivera-Nieves J, Olson T, Bamias G, Bruce A, Solga M, Knight RF, Hoang S, et al. L-selectin, alpha 4 beta 1, and alpha 4 beta 7 integrins participate in CD4+ T cell recruitment to chronically inflamed small intestine. J Immunol 2005;174:2343-2352.

31. Gorfu G, Rivera-Nieves J, Hoang S, Abbott DW, Arbenz-Smith K, Azar DW, Pizarro TT, et al. Beta7 integrin deficiency suppresses B cell homing and attenuates chronic ileitis in SAMP1/YitFc mice. J Immunol 2010;185:5561-5568.

32. Pastorelli L, Garg RR, Hoang SB, Spina L, Mattioli B, Scarpa M, Fiocchi C, et al. Epithelial-derived IL-33 and its receptor ST2 are dysregulated in ulcerative colitis and in experimental Th1/Th2 driven enteritis. Proc Natl Acad Sci U S A 2010;107:8017-8022.

33. Navaneethan U, Shen B. Hepatopancreatobiliary manifestations and complications associated with inflammatory bowel disease. Inflamm Bowel Dis 2010;16:1598-1619.

34. Mombaerts P, Iacomini J, Johnson RS, Herrup K, Tonegawa S, Papaioannou VE. Rag-1-Deficient Mice Have No Mature Lymphocytes-B and Lymphocytes-T. Cell 1992;68:869-877.

35. Takedatsu H, Mitsuyama K, Matsumoto S, Handa K, Suzuki A, Takedatsu H, Funabashi H, et al. Interleukin-5 participates in the pathogenesis of ileitis in SAMP1/Yit mice. Eur J Immunol 2004;34:1561-1569.

36. Floreani A, Rizzotto ER, Ferrara F, Carderi I, Caroli D, Blasone L, Baldo V. Clinical course and outcome of autoimmune hepatitis/primary sclerosing cholangitis overlap syndrome. Am J Gastroenterol 2005;100:1516-1522.

37. Seidel D, Eickmeier I, Kuhl AA, Hamann A, Loddenkemper C, Schott E. CD8 T cells primed in the gut-associated lymphoid tissue induce immune-mediated cholangitis in mice. Hepatology 2014;59:601-611.

38. Neumann K, Kruse N, Szilagyi B, Erben U, Rudolph C, Flach A, Zeitz M, et al. Connecting liver and gut: murine liver sinusoidal endothelium induces gut tropism of CD4+ T cells via retinoic acid. Hepatology 2012;55:1976-1984.

39. Eksteen B, Mora JR, Haughton EL, Henderson NC, Lee-Turner L, Villablanca EJ, Curbishley SM, et al. Gut homing receptors on CD8 T cells are retinoic acid dependent and not maintained by liver dendritic or stellate cells. Gastroenterology 2009;137:320-329.

40. Adams DH, Eksteen B. Aberrant homing of mucosal T cells and extra-intestinal manifestations of inflammatory bowel disease. Nat Rev Immunol 2006;6:244-251.

41. Matsuzaki K, Tsuzuki Y, Matsunaga H, Inoue T, Miyazaki J, Hokari R, Okada Y, et al. In vivo demonstration of T lymphocyte migration and amelioration of ileitis in intestinal mucosa of SAMP1/Yit mice by the inhibition of MAdCAM-1. Clin Exp Immunol 2005;140:22-31.

42. Crispe IN. Immune tolerance in liver disease. Hepatology 2014.

43. Derkow K, Muller A, Eickmeier I, Seidel D, Rust Moreira MV, Kruse N, Klugewitz K, et al. Failure of CD4 T-cells to respond to liver-derived antigen and to provide help to CD8 T-cells. PLoS One 2011;6:e21847.

44. Knolle PA, Uhrig A, Hegenbarth S, Loser E, Schmitt E, Gerken G, Lohse AW. IL-10 down-regulates T cell activation by antigen-presenting liver sinusoidal endothelial cells through decreased antigen uptake via the mannose receptor and lowered surface expression of accessory molecules. Clin Exp Immunol 1998;114:427-433.

45. Ishikawa D, Okazawa A, Corridoni D, Jia LG, Wang XM, Guanzon M, Xin W, et al. Tregs are dysfunctional in vivo in a spontaneous murine model of Crohn's disease. Mucosal Immunol 2013;6:267-275.